NASA TECHNICAL MEMORANDUM

NASA TM X-2144

NASA TM X-2144

EFFECT OF REACTOR IRRADIATION ON PROPERTIES OF A NONGALLING ALLOY

by Robert A. Hasse

Lewis Research Center
Cleveland, Ohio 44135

NATIONAL AERONAUTICS AND SPACE ADMINISTRATION • WASHINGTON, D. C. • DECEMBER 1970

1. Report No.	2. Government Accession No.	3. Recipient's Catalog No.
NASA TM X-2144		

4. Title and Subtitle	5. Report Date
EFFECT OF REACTOR IRRADIATION ON PROPERTIES OF A NONGALLING ALLOY	December 1970
	6. Performing Organization Code

7. Author(s)	8. Performing Organization Report No.
Robert A. Hasse	E-5704
	10. Work Unit No.
9. Performing Organization Name and Address	122-29
Lewis Research Center National Aeronautics and Space Administration Cleveland, Ohio 44135	11. Contract or Grant No.
	13. Type of Report and Period Covered
12. Sponsoring Agency Name and Address	Technical Memorandum
National Aeronautics and Space Administration Washington, D.C. 20546	14. Sponsoring Agency Code

15. Supplementary Notes

16. Abstract

The effect of reactor irradiation on Waukesha Metal 88, a nongalling alloy, was determined at fast neutron fluences up to 1×10^{21} neutrons/cm^2 (neutron energy > 1.0 MeV). Average specimen bulk temperature during irradiation was 355 K. The ultimate tensile strength increased by 120 percent and the 0.2 percent offset yield strength increased by 220 percent. The coefficient of sliding friction against 304 stainless steel was unaffected. The alloy swelled slightly during irradiation. Corrosion resistance of the alloy in contact with deionized water in-pile was good, although a slight susceptibility to crevice corrosion when mated with 304 stainless steel was noted.

17. Key Words (Suggested by Author(s))

Radiation effects
Sliding friction
Tensile properties
Bearing material
Waukesha 88

18. Distribution Statement

Unclassified - unlimited

19. Security Classif. (of this report)	20. Security Classif. (of this page)	21. No. of Pages	22. Price*
Unclassified	Unclassified	33	$3.00

*For sale by the National Technical Information Service, Springfield, Virginia 22151

EFFECT OF REACTOR IRRADIATION ON PROPERTIES OF A NONGALLING ALLOY

by Robert A. Hasse

Lewis Research Center

SUMMARY

The inherent galling properties of 304 stainless steel when mated with itself has been a problem in the NASA Plum Brook Reactor (PBR). A high nickel nongalling alloy, Waukesha Metal 88, was evaluated for use in a radiation environment as a mating material for stainless steel where sliding contact is required.

Tensile and wear test specimens were irradiated in the PBR up to a fast fluence of 1×10^{21} neutrons per square centimeter (neutron energy $E_n > 1.0$ MeV). Average specimen bulk temperature during irradiation was 355 K.

The hardness of the material increased from a Rockwell B of 80 to a Rockwell C of about 30. The density decreased slightly from 8.68×10^3 to 8.62×10^3 kilograms per cubic meter. The ultimate tensile strength and 0.2 percent offset yield strength increased 120 and 220 percent, respectively. The coefficient of sliding friction and wear rate when mated with 304 stainless steel were unaffected by the radiation. The corrosion resistance in the reactor environment was good except for some susceptibility to crevice corrosion.

It is concluded that this material is acceptable for use in the PBR at material temperatures up to 367 K and fast fluences up to 1×10^{21} neutrons per square centimeter ($E_n > 1.0$ MeV). The nongalling properties of the material are not affected under these conditions.

INTRODUCTION

The effect of irradiation on the properties of a nongalling alloy, Waukesha Metal 88, was determined. The specific properties measured were tensile strength, coefficient of sliding friction and wear rate sliding against 304 stainless steel, galling tendency

mated with 304 stainless steel, hardness, and density. The parameter studied was irradiation dose. Thermal controls were used to isolate temperature effects.

The tendency of stainless steel to gall or seize when mated with itself has been a problem at the NASA Plum Brook Reactor (PBR). Typical of the problems is the galling of the 304 stainless steel locking nuts on the control rods and the stainless steel nuts on the core grid locking mechanism. A nongalling material was therefore required for such applications. Also, a material to serve as a sliding contact against the 304 stainless steel clad control rods was required on the core grid (control rod guide blocks).

A set of selection criteria was established for a suitable nongalling material. The subject material was then chosen in accordance with these criteria. The program described in this report was designed and conducted to determine the effects of irradiation on the important properties of this material.

SYMBOLS

d days

E_i lowest neutron energy

E_n energy of neutron

f coefficient of sliding friction, frictional force/normal load

N* total number of samples

$\bar{n}$* average value of N samples

ni value for individual sample i

S estimator of σ (standard deviation), $\left[\sum_{1}^{N} \frac{(\bar{n} - ni)^2}{N - 1}\right]^{1/2}$ for $N < 10$ and

$\left[\sum_{1}^{N} \frac{(n - ni)^2}{N}\right]^{1/2}$ for $N \geq 10$

V volume

ρ density

φ neutron flux

MATERIAL

The material tested was Waukesha Metal 88, a nongalling alloy. Waukesha 88 is a high nickel alloy containing a dispersion of a bismuth-tin (Bi-Sn) alloy that acts as a lubricant. The chemical composition of this alloy is given in table I, and the physical and mechanical properties of the alloy are given in table II.

Corrosion Resistance

Prior to the final selection of the alloy, a corrosion test was performed. Samples of the material were placed in deionized water in an autoclave. The temperature was maintained at 422 K for 56 days. Based on specimen weight loss, the corrosion rate was less than 0.05 mil per year (1.27×10^{-8} m/yr). The water was analyzed for components of the alloy, and all were below detection limits. A metallographic examination of the specimens showed no evidence of corrosive attack. Based on these results, it was concluded that the material had adequate corrosion resistance to be tested in the PBR primary system. Further evaluation was made on the irradiated specimens since irradiation can affect the corrosion properties of some materials.

TABLE I. - COMPOSITION OF

WAUKESHA METAL 88

Element	Amount, wt. %	
	From manufacturer's literature	From certified analysis
Ni	Balance	74.49
Fe	[a]2.0	.48
Cr	11 to 14	13.25
Mo	2.5 to 3.5	2.34
Bi	3.0 to 5.0	3.62
Sn	3.0 to 5.0	4.46
Mn	.65 to 1.0	.85
Si	.15 to 0.50	.49
C	[a].05	.02

[a]Maximum.

TABLE II. - PHYSICAL AND MECHANICAL PROPERTIES OF WAUKESHA METAL 88

Property	From manufacturer's literature	From measurements in PBR
Tensile strength, psi (N/m^2)	[a]40 000 (2.78×10^8)	52 100 (3.59×10^8)
0.2 Percent offset yield strength, psi (N/m^2)	[a]33 500 (2.31×10^8)	37 100 (2.56×10^8)
Elongation, percent	6	13.4
Hardness	140 to 160 (Brinnel hardness number, 3000 kg, 10 mm)	80 (Rockwell B)
Density, kg/m^3	8.6×10^3	8.68×10^3
Coefficient of sliding friction (dry)		
On chrome plate at load of 512 psi (3.52×10^6 N/m^2)	0.33	
On 18-8 stainless steel at load of 512 psi (3.52×10^6 N/m^2)	0.23	
On 304 stainless steel at load of 29 psi (2.00×10^5 N/m^2)		0.40

[a]Minimum.

Nuclear Properties

It was the purpose of this program to determine the nuclear properties of the alloy. It was apparent, however, that only one component of the alloy could lead to an undesirable activation product in the primary cooling water (PCW). The Bi would transmute to the α-particle emitting isotope polonium-210 (Po^{210}). The presence of α emitters can complicate the disposal of waste water because of their low maximum permissible concentration (MPC) limits in the plant effluent. The PCW was analyzed for the presence of Po^{210} during the irradiation phase of this program. These analyses showed it to be below detection limits and the MPC.

IRRADIATION

Irradiation Facility

The test specimens were irradiated in lattice position 5 (LA-5) of the NASA PBR. The PBR is a 60-megawatt (thermal) light water moderated and beryllium reflected test reactor. A horizontal section of the core is shown in figure 1. A full description of the PBR is given in reference 1.

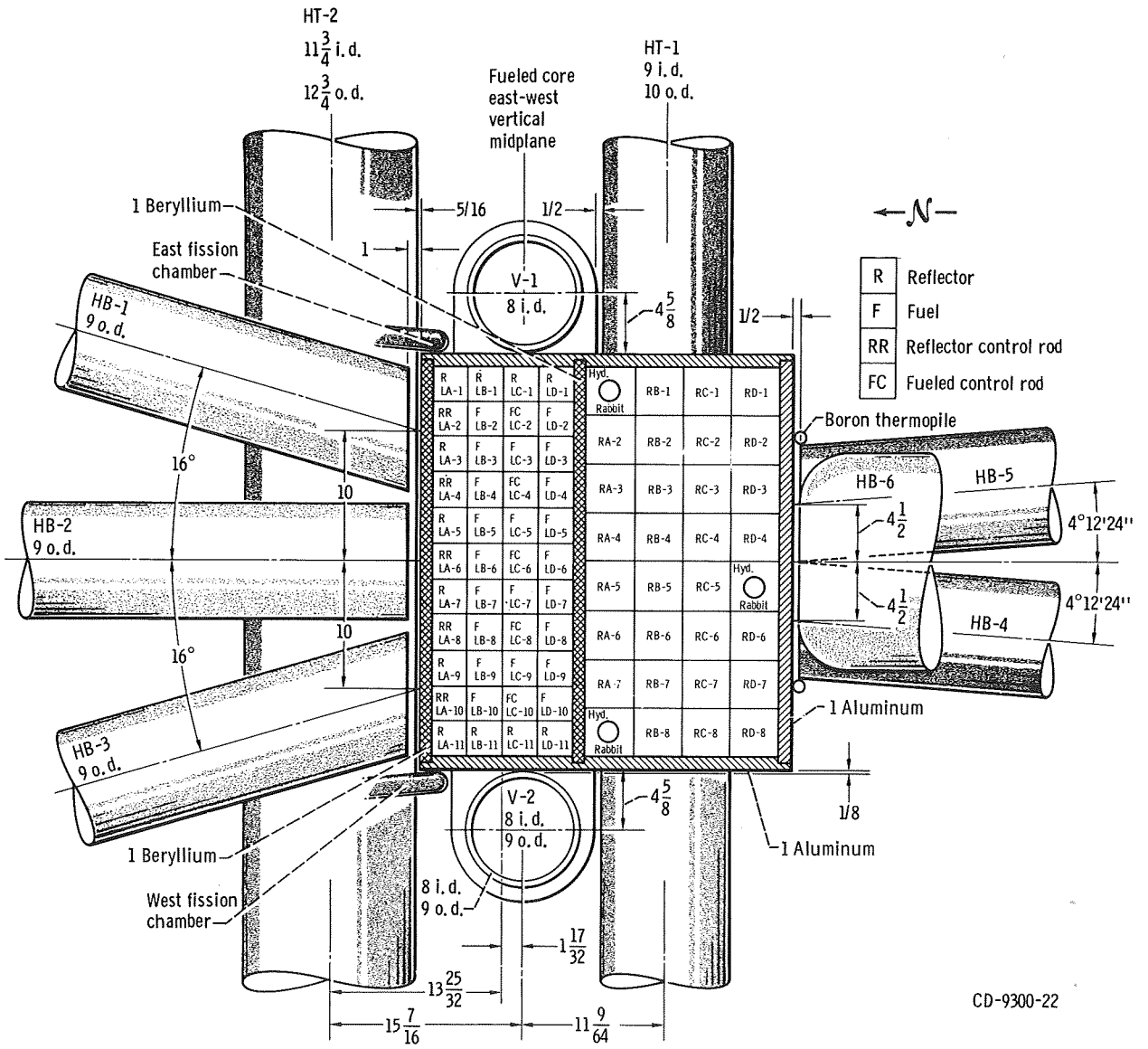

Figure 1. - Horizontal section of reactor core. (All linear dimensions are in inches.)

Irradiation Capsule

A standard PBR L position capsule was used for these irradiations. The body of the capsule is composed of 10 separate cylindrical segments, each capable of holding six specimens (fig. 2). The specimens are loaded on a spindle assembly and placed in the body segment as shown in figure 2. Primary cooling water flows through the capsule interior cooling the specimens directly.

Each body segment contains three sets of two dosimeter wire wells spaced at 120° intervals. One thermal flux and one fast flux dosimeter are present in each set of wells during irradiation. (Dosimetry details are given in the appendix.)

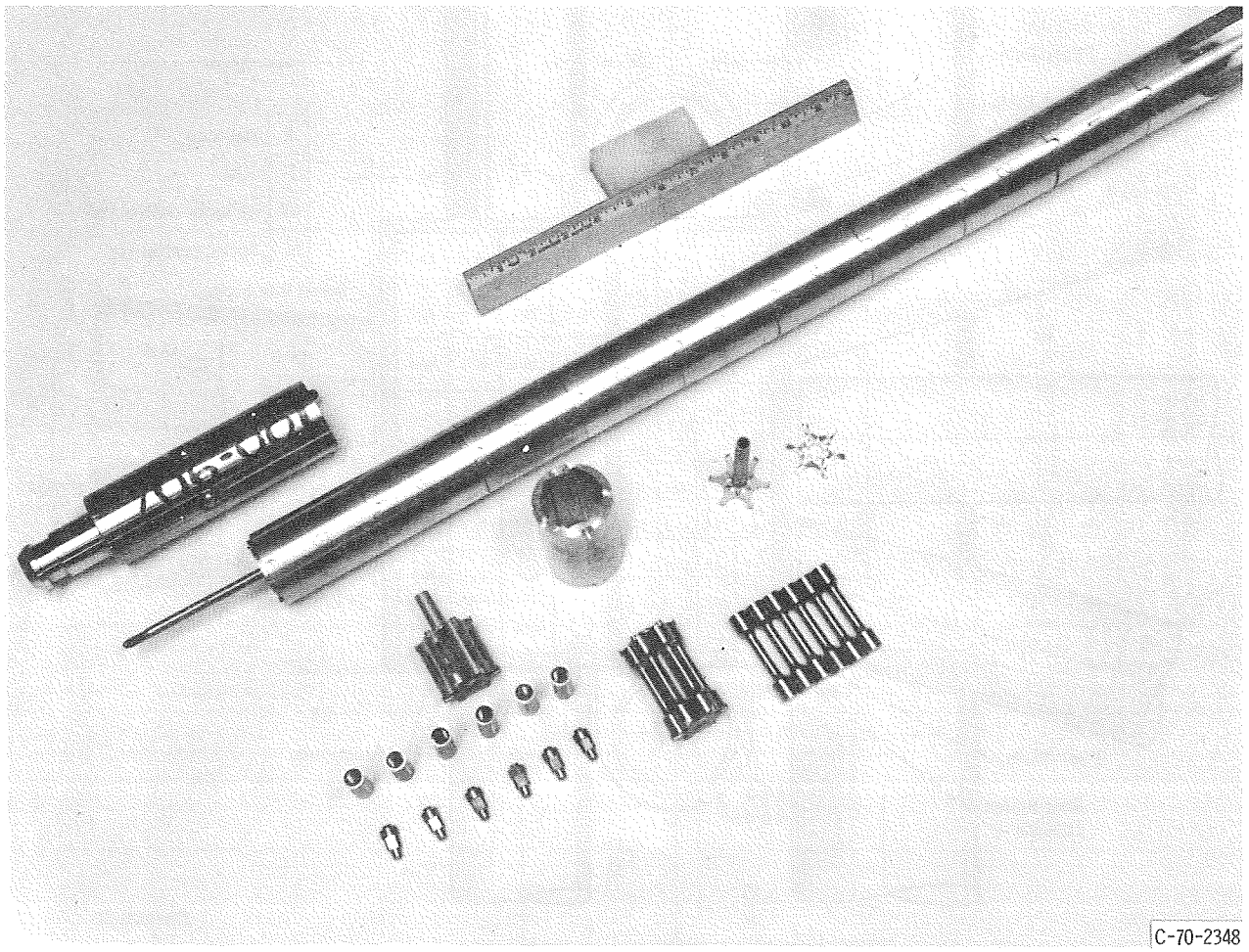

Figure 2. - Capsule assembly.

Environment

The specimens were in direct contact with the PCW during irradiation. A summary of the irradiation environment is given in table III.

TABLE III. - IRRADIATION ENVIRONMENT

Factor	Nominal value	Range
PCW conductivity, μmho/cm^3	0.8	0.7 to 0.9
PCW pH	6.3	---------
PCW pressure, psig (N/m^2)	160 (1.12×10^6)	
PCW temperature, K	338	---------
Specimen average bulk temperature, K	355	349 to 360
Thermal flux (fuel cycle average),[a] φ_{th}, neutrons/(cm^2)(sec)	3.7×10^{14}	0.8 to 6.6×10^{14}
Fast flux (fuel cycle average >1.0 MeV),[a] φ_f, neutrons/(cm^2)(sec)	6.4×10^{13}	0.15 to 1.13×10^{14}
γ heating, W/g	9	13 to 4.5

[a]Detailed treatment of neutron dosimetry and neutron energy spectrum are given in the appendix.

EXPERIMENTAL METHODS

Test Specimens

Two types of specimens were tested, tensile and wear (coefficient of sliding friction). The tensile specimens used were ASTM standard specimens (ASTM E8-61T). The total length was 2.5 inches (6.35 cm), the gage length was 1.0 inch (2.54 cm), and the gage diameter was 0.25 inch (0.635 cm).

The wear test specimen is shown in figure 2. The test end was hemispherical with a 0.125-inch (0.318-cm) spherical radius. The opposite end was threaded. A 304 stainless steel nut was torqued onto the threaded end prior to irradiation. This assembly was then placed in a slotted aluminum tube and placed in the spindle assembly. The aluminum tube served as a holding fixture for the specimens in the spindle assembly.

Test Apparatus

The tensile tests were conducted with a 10 000-pound (4536-kg) test machine. A schematic of the method used to determine the coefficient of sliding friction and the wear rate is shown in figure 3. A photograph of the equipment is shown in figure 4.

Test Procedures

At predetermined intervals, the irradiation capsule was removed from the reactor and transferred to the PBR Hot Laboratory for specimen removal and testing. Dosimeter wires were also removed and replaced at this time. The capsule and remaining specimens were then returned to the reactor for continued irradiation. The specimens were removed in groups of three each. The specimens in each group had approximately equal neutron doses.

Two sets of control specimens were used. Specimens of one set, called ambient controls, were kept in air at room temperature. Specimens of the second set were re-

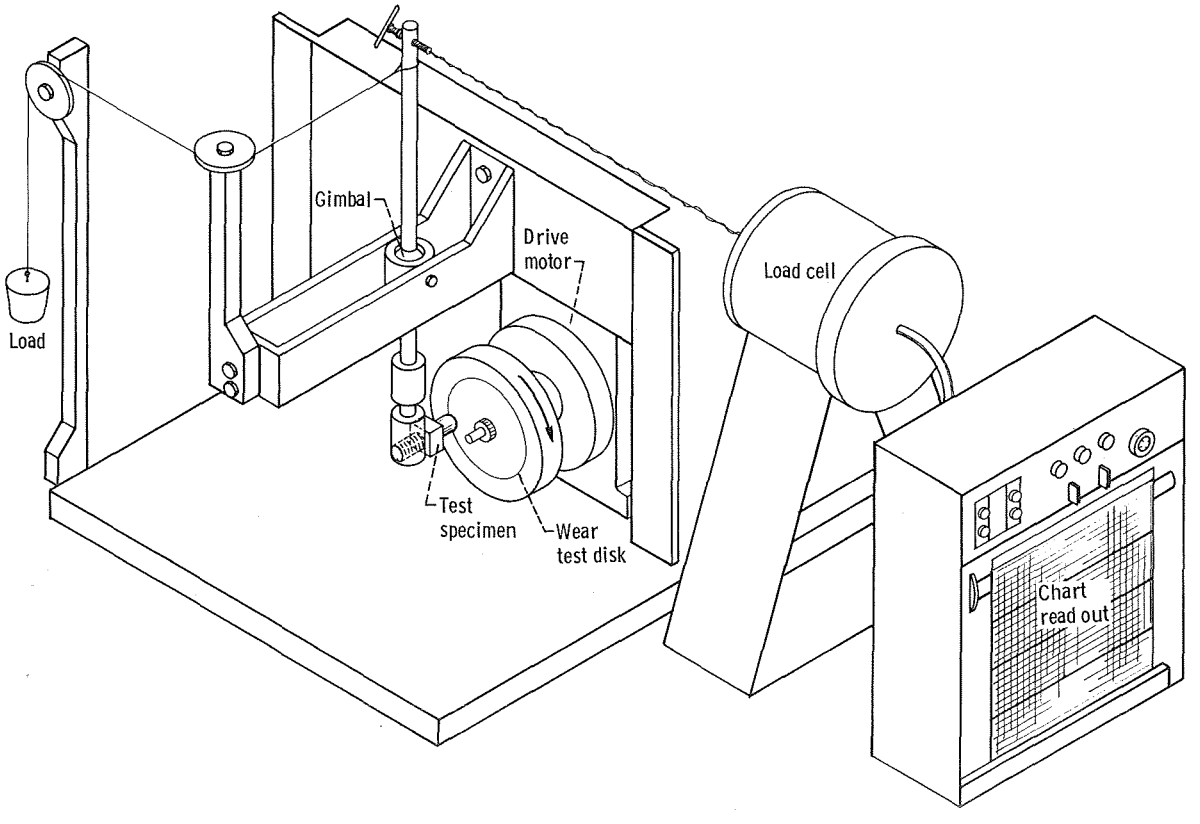

Figure 3. - Schematic of rig used to determine coefficient of sliding friction (wear test rig).

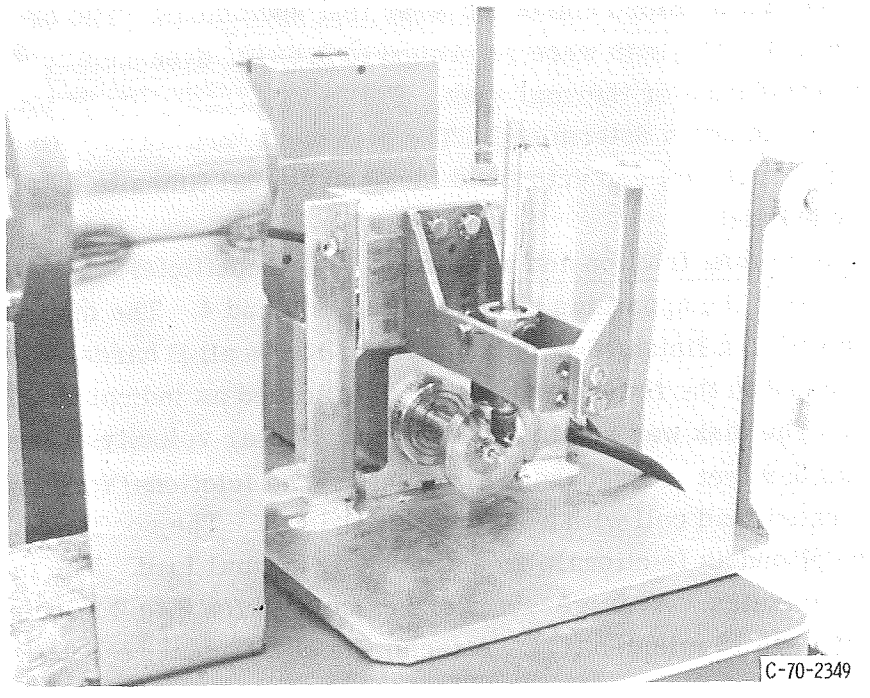

Figure 4. - Wear test apparatus.

ferred to as thermal controls. These were kept in deionized water at 367 K for an interval matching the irradiation period of selected specimen groups. The temperature approximated that of the irradiated specimens during irradiation. Also, the temperature of the water was cycled to duplicate that of the irradiated specimens during reactor shutdowns. The testing of all control specimens was interspersed with the testing of the irradiated specimens.

Physical measurements. - The density and hardness were determined for all tensile specimens before and after irradiation or thermal soak. Further measurements made on the ambient controls were interspersed with measurements of the irradiated and thermal control specimens. The hardness determinations were made with a Rockwell Hardness Tester using the 1/16-inch (0. 16-cm) Braile indenter and a 30-kilogram load. Densities were determined by the immersion method using an analytical balance (0. 2 mg sensitivity) and carbon tetrachloride. The physical measurements were made prior to tensile testing.

The weights of the wear specimens were determined before and after irradiation or thermal soak and after the wear test using the analytical balance.

Tensile tests. - Following the physical measurements, the tensile specimens were tested to failure at a strain rate of 0. 2 inch per minute (0. 51 cm/min). Total elongation was determined directly from the chart readout of the test machine.

Galling tests. - A 304 stainless steel nut was torqued to 5.6×10^7 dyne-centimeters (5.6×10^2 N-cm) on the threaded end of the wear test specimens. The breakaway torque was then determined. The nuts were retorqued to 5.6×10^7 dyne-centimeters (5.6×10^2 N-cm) prior to irradiation or thermal soak. Following irradiation or thermal soak the breakaway torque was again determined. The nuts were then torqued to 5.6×10^7 dyne-centimeters (5.6×10^2 N-cm) and untorqued three additional times to determine if any galling tendency existed.

Coefficient of sliding friction and wear rate. - The coefficient of sliding friction was determined using the apparatus shown in figures 3 and 4. The disk was 304 stainless steel machined to a finish of 32 rms and had a Rockwell B hardness of 66. The specimen was placed in the fixture and dead weight loaded as indicated. The normal load was 160 grams. The disk was rotated at 900 rpm. Linear velocity of the point of specimen contact was 5.9 feet per second (1.8 m/sec). The frictional force was determined by using a calibrated load cell with a strip chart readout. The coefficient of sliding friction f was defined as frictional force divided by normal load. The test was normally run for 15 minutes. Average f's were calculated for 0 to 2 minutes (f_1), 10 to 15 minutes (f_2), and 0 to 15 minutes (f_A). A facsimile of a typical readout from the load cell is shown in figure 5.

Following the test, the specimens were weighed to determine their weight loss. The weight loss represented the total wear during the test and, for equal test times, was proportional to the wear rate. No attempt was made to calculate actual wear rates since the specimen surface area varied during the test because of the hemispherical end.

Metallography. - A metallographic examination was performed on selected control and irradiated specimens. Photomicrographs were taken at magnifications of 250 and 500 in the as-polished condition. The specimens were then etched with aqua regia and rephotographed at the same magnifications.

Autoradiography of wear disks. - Bismuth transmutes to an α emitting isotope, polonium-210, in a thermal neutron flux. This provides a unique opportunity to determine the distribution of the lubricating Bi-Sn alloy on the wear test disks used with the irradiated specimens. The reaction producing the Po^{210} is

$$Bi^{209}(n,\gamma)Bi^{210} \xrightarrow[5.0\ d]{\beta^-} Po^{210} \xrightarrow[138.4\ d]{\alpha} Pb^{206}(s)$$

Cellulose nitrate is sensitized to a sodium hydroxide etch by exposure to heavily ionizing radiation (α particles, fission fragments). Its relative insensitivity to β^- and γ-ray exposure permits the determination of the distribution of α emitting isotopes in the presence of a β-γ field. Cellulose nitrate films were exposed directly to selected

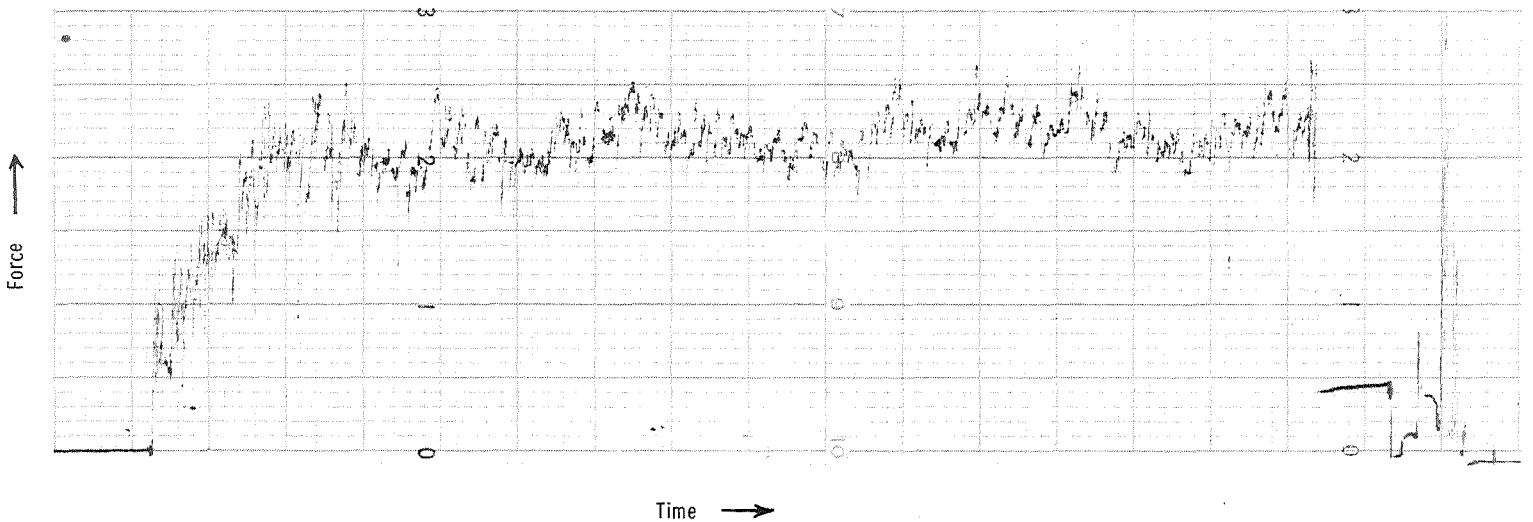

Figure 5. - Facsimile of wear test readout.

wear test plates and then etched in NaOH. Exposure times varied from 6 to 12 hours depending on the length of specimen neutron exposure. Etch times were approximately 15 minutes.

The same plates were then placed on Polaroid film using the film pack cover as an α absorber. The resultant exposure indicated the distribution of the β-γ activity on the wear test plate. The contribution from β-γ activity associated with the Bi-Sn alloy was less than 2 percent. Comparison of these exposures to the cellulose nitrate exposures showed the relative distribution of the lubricating alloy and the base metal.

RESULTS AND DISCUSSION

General Examination

Following irradiation or thermal soak, all specimens were wiped with a soft cloth to remove any loose deposits and visually examined. Some specimens showed a light adherent deposit on their surfaces (figs. 6 and 7). This deposit is frequently observed on specimens irradiated in contact with the PCW. Although these specific deposits were not analyzed, previous analyses have shown them to be a mixture of aluminum and beryllium oxide. The deposits were considered too superficial to affect the measured physical or mechanical properties. Therefore, no attempt was made to remove them.

The irradiated wear test specimens showed evidence of pitting on the bottom thread (fig. 8(a)). This was not observed on the thermal controls (fig. 8(b)). The pitting was interpreted as galvanic or crevice type corrosion. The water in this area would be relatively stagnant, and two somewhat dissimilar metals are in contact. The fact that no evidence of corrosive attack was observed in previous tests with uncoupled Waukesha 88 also lends credence to this interpretation. Stress corrosion was discounted by general appearance and the fact that the attack did not occur preferentially at the thread root, where the stress is concentrated.

The lack of attack on the thermal controls could be due to the differences in flow patterns and water quality and perhaps the lack of a radiation environment. The flow over the irradiated specimens was from top to bottom, which allowed the specimen shoulder to act as a breakwall or flow deflector. This would permit some stagnation in the vicinity of the thread. The flow over the thermal controls was lateral, and the specimens were not rigidly mounted. Less stagnation would be expected in this case. Radiation can accelerate the corrosion rate of some materials under certain conditions (ref. 4). Its effect is dependent on the material, water quality, temperature, and type of corrosion. It is impossible to assess its contribution in this case without further studies.

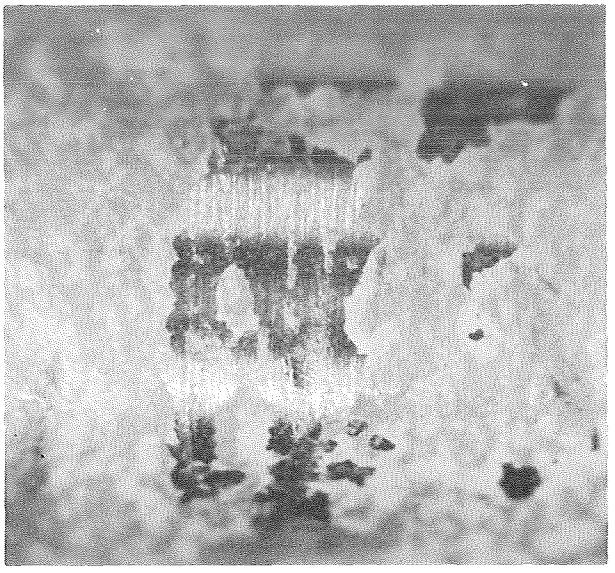

(a) Specimen 213; X12.

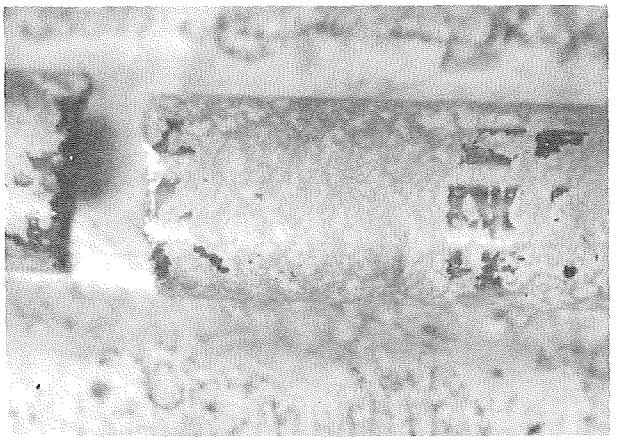

(b) Specimen 213; X4.

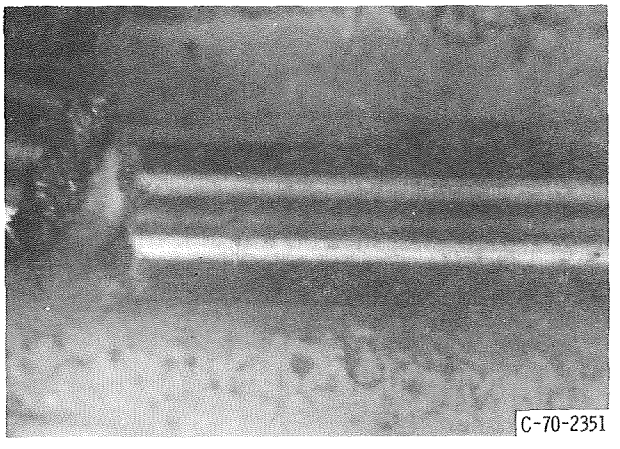

(c) Specimen 205; X4.

Figure 6. - Comparison of deposits on irradiated tensile specimens.

The general corrosion resistance of this material in contact with the PCW is very good. However, its apparent susceptibility to crevice corrosion when mated with 304 stainless steel must be considered when potential applications are evaluated.

Physical Properties

The physical properties of the tensile specimens were measured prior to tensile testing. An increase in hardness and a slight decrease in density were observed for the irradiated specimens.

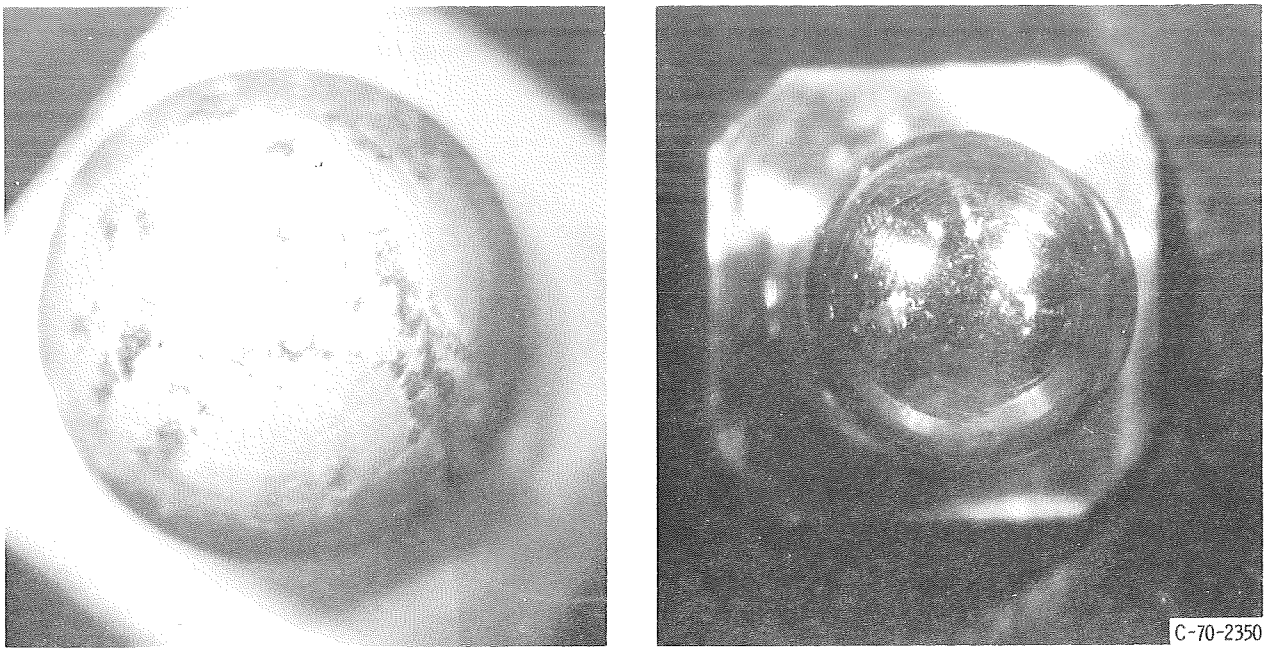

(a) Specimen 104. (b) Specimen 143.

Figure 7. - Comparison of deposits on irradiated wear test specimens.

Hardness. - The hardness of the material increased somewhat more dramatically than expected (table IV). The increase was from a Rockwell B (R_B) of 80 to approximately 104. The R_B of 104 is equivalent to a R_C hardness of approximately 30. The hardness increase appeared to have saturated at a fast fluence of approximately 1×10^{20} neutrons per square centimeter ($E_n > 1.0$ MeV). However, the post irradiation hardness exceeded the recommended range for the R_B scale and accuracy was lost. A small amount of additional hardening probably occurred, as indicated by the further increase in tensile strength.

Density. - An apparent small density decrease from 8.68×10^3 to 8.62×10^3 kilograms per cubic meter was observed. Small decreases in density at modest fluences have been reported before (refs. 2 and 3). Others feel that these observations are probably due to experimental error (ref. 4), except for refractory metals, for which lattice parameter measurements have confirmed the change (ref. 5). Since slight swelling can cause problems in some applications (ref. 1), some discussion of the present results is justified.

Swelling at modest fluences does have a basis in theory. The density decrease is predicted by simple vacancy-interstitial pair generation within the crystal (ref. 6). Although the interstitial causes an expansion and the vacancy a contraction, the absolute magnitude of the interstitial effects is about five times that for the vacancy. The result is a net expansion. Because of vacancy-interstitial recombinations during irradiation, this expansion would approach some peak value as exposure increases. A reversal of

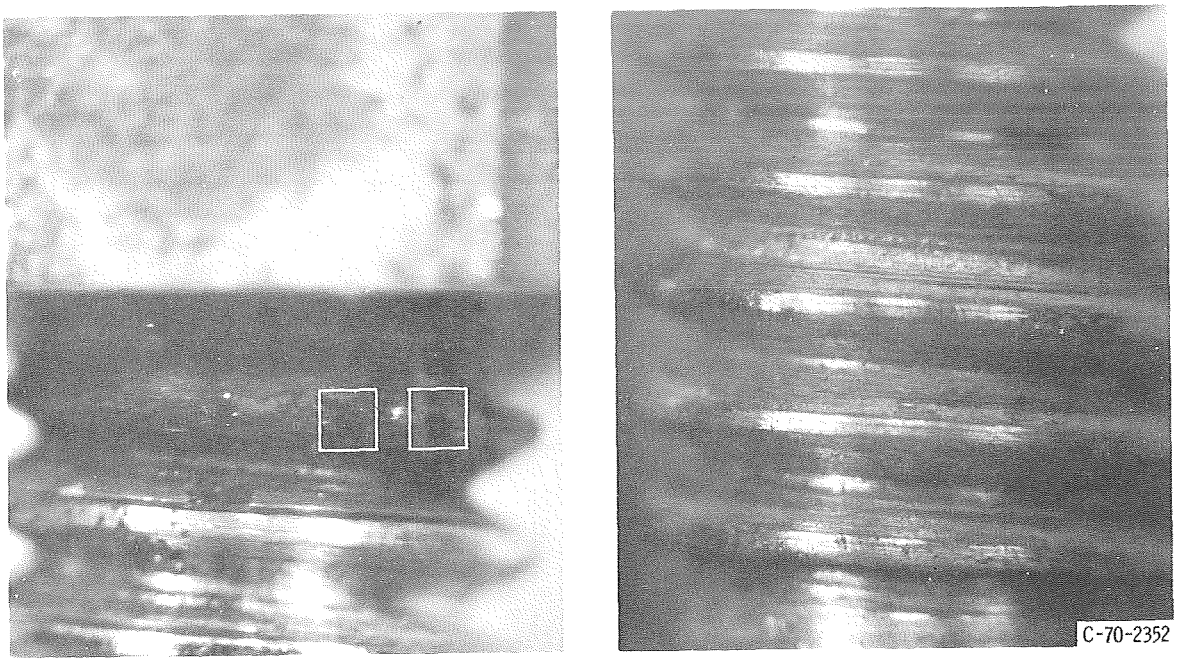

(a) Irradiated speciemn 101.

(b) Thermal control specimen 121.

Figure 8. - Wear test specimen threads. X12.

the swelling process has also been observed (ref. 5). This is explained by the fact that the energy of migration for the interstitial is one-fifth to one-tenth of that for a vacancy. Thus, if the temperature is high enough, the interstitials would migrate to trapping sites where they are less effective in producing swelling, while the vacancies would remain relatively immobile. Ultimately, then, the effect of the vacancies would predominate, and a reversal of the swelling process would occur.

Experimental error can be ruled out in the present measurements by examining the data for the control specimens. The densities of all control and test specimens were measured prior to irradiation of the test specimens. Further density measurements of the control specimens were interspersed throughout the postirradiation measurements of the irradiated specimens. The greatest difference in the density measured for any control specimen was 0.02×10^3 kilograms per cubic meter (1 specimen) and 0.01×10^3 kilograms per cubic meter or less for the remainder (11 specimens). One can be at least 95 percent confident then that any change greater than 0.02×10^3 kilograms per cubic meter is real.

Accepting that the observed density change is real, one must rule out causes other than material swelling. The deposit present on these specimens presents the only identifiable source of potential error. Assuming a density as low as 10^3 kilograms per cubic meter for the deposit, at least 36 milligrams of deposit would be required to cause the decrease observed. Using a more reasonable density for an Al-Be oxide (2.3×10^3

kg/m^3), the total deposit needs to exceed 80 milligrams to cause the decrease to 8.62×10^3 kilograms per cubic meter.

It should be noted at this point that the difference in preirradiation and postirradiation weights is not a measure of the weight of the deposit. Since some specimens actually lost weight, some loss of the base material can occur. This can be caused by erosion or chipping of specimen edges during handling.

The volume fractions of base material and deposit can be calculated assuming no change in the density of the base material by the following equation:

$$\rho_1 V_1 + \rho_2 V_2 = \rho_o V_t$$

where

ρ_1 density of base material, 8.68×10^3 kg/m^3

V_1 volume of the base material

ρ_2 density of deposit

V_2 volume of deposit

ρ_o observed density of system

V_t total volume of system

This equation reduces to

$$\rho_1 V_1 + \rho_2 V_t - \rho_2 V_1 = \rho_o V_t$$

since

$$V_1 + V_2 = V_t$$

If a value for ρ_2 is assumed, the only unknown is V_1. By assuming a value of 2.0×10^3 kilograms per cubic meter for ρ_2 for a system with ρ_o of 8.62×10^3 kilograms per cubic meter, a volume fraction of base material of 0.991 and of deposit of 0.009 is obtained. Also, a change in volume fraction of deposit of approximately 40 percent would cause a change in ρ_o of 0.02×10^3 kilograms per cubic meter. Considering the excellent agreement of postirradiation density measurements within specimen groups and, excluding group G, between groups, one must assume that the volume fraction of deposit varied no more than 25 percent. This is quite contrary to visual observations (see figs. 6 and 7). One is led to the conclusion, therefore, that some decrease in the density of the base material did occur. Although some contribution from the deposit cannot be

ruled out, it should be noted that a deposit of less than approximately 0.2 volume percent and a density of around 2.0×10^3 kilograms per cubic meter would not show a measurable effect on the observed density as compared to the preirradiation density.

Tensile Properties

The changes in tensile properties are given in tables IV and V. The ultimate strength increased by 120 percent and the 0.2 percent offset yield strength by 220 percent. Total elongation essentially disappeared.

The mechanisms of radiation strengthening of materials have been discussed extensively elsewhere (ref. 4) and will not be detailed here. The changes in tensile properties observed for Waukesha 88 in this work would have no deleterious effect for intended applications.

Galling Tests

The results of the galling tests are given in table VI. The breakaway torque was increased slightly during irradiation and the thermal soak. This indicates that most of this increase was due to the thermal exposure, light deposits, or corrosion on the threads. The effect appears to be permanent and does not increase with exposure. The slightly larger increase for the irradiated specimens indicates that the effect is radiation enhanced possibly because of the swelling of the irradiated material.

The initial breakaway torque after irradiation for the group F specimens seems anomalous. The subsequent torque-untorque operations showed no difference from the other specimens. It is concluded, therefore, that the nuts became loosened prior to the initial breakaway torque determination after irradiation. The specimens were initially torqued (prior to irradiation) in numerical order. It is not likely, therefore, that errors in initial torque pressure occurred. Thermal control group TC-2 specimens had the same thermal exposure as these specimens and were processed at the same time. The only difference, then, is the radiation dose. One mechanism would be a slight redensification of the Waukesha alloy at this higher dose. An initial swelling might have backed the nut off slightly and subsequent redensification left it loosened.

From a qualitative standpoint, no galling or seizing tendencies could be detected during these tests.

TABLE IV. - PHYSICAL AND MECHANICAL PROPERTIES OF IRRADIATED TENSILE SPECIMENS

Group	Specimen	Fast fluence ($E_n > 1.0$ MeV), neutrons/cm^2 (a)	Thermal fluence, neutrons/cm^2 (a)	Irradiation time, hr	Specimen weight, kg		Density, kg/m^3		Rockwell B hardness		Ultimate strength, [b]	
					Preirradiation	Postirradiation	Preirradiation	Postirradiation	Preirradiation	Postirradiation	ksi	N/m^2
G	210	1.0×10^{20}	7.4×10^{20}	910	38.5774×10^{-3}	38.5776×10^{-3}	8.68×10^{3}	8.64×10^{3}	81	104	82.3	5.67×10^{8}
	212	.9	7.0	910	38.5046	38.5049	8.68	8.64	78	102	94.0	6.48
	214	1.0	7.2	910	37.8924	37.8890	8.68	8.64	82	105	74.7	5.15
H	204	2.6×10^{20}	15×10^{20}	910	37.9777×10^{-3}	37.9772×10^{-3}	8.68×10^{3}	8.64×10^{3}	78	106+	114	7.85×10^{8}
	206	2.2	15	910	37.9607	37.9604	8.68	8.63	80	104	93.0	6.40
	208	2.7	15	910	38.1358	38.1341	8.68	8.63	81	106+	94.0	6.48
I	211	2.4×10^{20}	20×10^{20}	2535	38.3334×10^{-3}	38.3347×10^{-3}	8.69×10^{3}	8.63×10^{3}	78	104	114	7.85×10^{8}
	213	2.3	19	2535	38.1507	38.1678	8.68	8.62	84	105	115	7.93
	215	2.4	19	2535	38.0852	38.0967	8.68	8.62	78	105	115	7.93
J	201	6.6×10^{20}	40×10^{20}	4149	38.3405×10^{-3}	38.3494×10^{-3}	8.68×10^{3}	8.62×10^{3}	78	104	125	8.61×10^{8}
	202	6.9	39	4149	38.0898	38.0979	8.68	8.62	80	105	121	8.35
	203	7.1	41	4149	38.1111	38.1187	8.68	8.62	82	105	119	8.20
K	205	9.8×10^{20}	64×10^{20}	4149	38.4745×10^{-3}	38.4597×10^{-3}	8.68×10^{3}	8.63×10^{3}	77	102	115	7.93×10^{8}
	207	11	63	4149	38.2143	38.2006	8.68	8.63	80	105	120	8.27
	209	11	66	4149	38.3297	38.3121	8.69	8.63	78	105	118	8.13

[a] Dosimetry details and uncertainties are given in appendix.

[b] 0.2 Percent offset yield strength was undetectable; total elongation was less than 1 percent for all specimens.

TABLE V. - PHYSICAL AND MECHANICAL PROPERTIES OF TENSILE CONTROL SPECIMENS

Group	Specimen	Soak time at 367 K, hr	Specimen weight, kg		Density, kg/m^3		Rockwell B hardness		Ultimate strength,		0.2 Percent offset yield strength,		Total elongation, percent
			Preirradiation	Postirradiation	Preirradiation	Postirradiation	Preirradiation	Postirradiation	ksi	N/m^2	ksi	N/m^2	
TC-3	216	2535	38.1413×10^{-3}	38.1411×10^{-3}	8.67×10^3	8.66×10^3	80	83	63.7	4.39×10^8	45.8	3.16×10^8	15.4
	217	2535	38.5490	38.5494	8.68	8.67	80	82	60.9	4.19	44.2	3.04	13.6
	218	2535	38.3149	38.3153	8.67	8.67	75	79	62.3	4.39	44.2	3.04	17.2
TC-4	219	4149	37.8953×10^{-3}	37.9000×10^{-3}	8.67×10^3	8.66×10^3	76	77	60.0	4.13×10^8	42.2	2.90×10^8	13.8
	220	4149	38.5496	38.5502	8.68	8.67	81	79	58.3	4.02	43.2	2.97	11.7
	221	4149	38.0350	38.0407	8.68	8.66	79	77	60.0	4.13	41.8	2.88	15.8
Average 2S and symmetry[a]	---	----	-------	-------	8.68×10^3	8.67×10^3	--	--	60.9	4.19×10^8	43.6	3.00×10^8	14.6
	---	----	-------	-------	--------	--------	--	--	3.8	.26 (2/3)	2.9	.20 (3/3)	3.9 (3/3)
AC-2	222	Ambient	38.1939×10^{-3}	38.1938×10^{-3}	8.67×10^3	8.68×10^3	79	81	47.6	3.28×10^8	33.2	2.29×10^8	13.5
	223	↓	37.9325	38.9323	8.68	8.69	78	80	52.0	3.58	36.3	2.50	16.0
	224		38.1161	38.1141	8.67	8.67	81	80	48.5	3.34	36.6	2.52	8.9
	225		37.9767	37.9762	8.68	8.68	81	80	57.7	3.97	41.2	2.82	12.8
	226		38.5421	38.5420	8.67	8.68	81	79	57.6	3.97	43.2	2.97	11.8
	227		38.5857	38.5855	8.67	8.68	81	79	49.0	3.38	32.5	2.24	17.6
Average 2S and symmetry[a]	---	--------	-------	-------	8.67×10^3	8.68×10^3	--	--	52.1	3.59×10^8	37.1	2.56×10^8	13.4
	---	--------	-------	-------	--------	--------	--	--	9.1	.63 (2/4)	8.5	.59 (2/4)	6.2 (3/3)

[a]Number of specimens above average/number of specimens below.

TABLE VI. - BREAKAWAY TORQUE[a]

Group	Specimen	Breakaway torque,[b] dyne-cm ($N\times10^5$-cm)						
		Preirradiation	Postirradiation					
			First measurement	Second measurement	Third measurement	Fourth measurement	Specimen average	Group average
A	143	------	62×10^6	51×10^6	56×10^6	45×10^6	53×10^6	50×10^6
	144	------	51	45	45	45	47	
B	101	38×10^6	53×10^6	56×10^6	53×10^6	54×10^6	54×10^6	55×10^6
	103	37	62	56	53	54	56	
	105	36	64	52	51	53	55	
C	107	39×10^6	61×10^6	54×10^6	54×10^6	51×10^6	55×10^6	53×10^6
	109	39	55	52	51	51	52	
	111	36	56	51	48	46	50	
D	102	37×10^6	62×10^6	56×10^6	55×10^6	56×10^6	57×10^6	52×10^6
	104	34	52	51	51	48	51	
	106	42	53	51	52	51	52	
E	113	38×10^6	54×10^6	53×10^6	52×10^6	52×10^6	53×10^6	52×10^6
	114	37	51	52	53	53	52	
	115	38	51	52	52	51	52	
F	108	39×10^6	37×10^6	50×10^6	53×10^6	51×10^6	51×10^6	[c]52×10^6
	110	34	25	52	51	53	52	
	112	39	34	56	48	51	52	
TC-1[d]	116	39×10^6	45×10^6	45×10^6	45×10^6	51×10^6	47×10^6	48×10^6
	117	39	47	48	50	48	48	
	118	40	50	50	48	50	50	
TC-2[d]	119	40×10^6	42×10^6	45×10^6	51×10^6	51×10^6	47×10^6	47×10^6
	120	45	43	42	46	47	45	
	121	42	50	47	51	51	50	
Average for all specimens	---	39×10^6	------	------	------	------	------	------

[a]Fluences and soak times are given in table VII.

[b]Nuts were torqued to 56×10^6 dyne-cm.

[c]Initial postirradiation measurement excluded from averages.

[d]Thermal control values are for pre- and postthermal soak.

Coefficient of Sliding Friction

Coefficients of sliding fraction f for the test specimens are given in tables VII and VIII and figure 9. The normal load during testing was 160 grams. The specific load after 15 minutes approximated 29 pounds per square inch.

As can be seen in figure 9(c) the f_A for all specimens fell within the 2S uncertainty band for the ambient control specimens except for one specimen. The distribution of the irradiated specimens about the control average was symmetrical (number above average/number below average, 9/8). Also, the average f_A of all irradiated specimens and its uncertainty did not differ significantly from those of the ambient control specimens. One concludes, therefore, that no measurable change occurs in f_A, at least up to a dose of approximately 1×10^{21} neutrons per square centimeter ($E_n > 1.0$ MeV). The

TABLE VII. - COEFFICIENT OF SLIDING FRICTION FOR CONTROL SPECIMENS

Group	Specimen	Soak time at 367 K, hr	Total f test run time, min	Coefficient of sliding friction[a]			Weight loss, kg
				f_1	f_2	f_A	
TC-1	116	2535	15.0	0.20	0.33	0.31	[b] 18.8×10^{-3}
	117	2535	15.0	.28	.38	.35	13.1
	118	2535	15.0	.20	.33	.28	14.3
TC-2	119	4149	15.0	0.22	0.40	0.33	13.0×10^{-3}
	120	4149	15.0	.30	.43	.39	12.9
	121	4149	15.0	.29	.47	.43	11.9
Average[c] for TC-1 and TC-2	---	----	----	0.25	0.39	0.35	13.0×10^{-3}
2S[c] and symmetry[d]	---	----	----	.09 (3/3)	.11 (2/4)	.10 (2/4)	1.7 (2/2)
AC-1	123	Ambient	20.4	0.28	0.38	0.36	[b] 28.2×10^{-3}
	124	↓	15.3	.31	.38	.38	11.6
	128		15.0	.31	.47	.45	12.5
	129		15.0	.34	.47	.45	12.2
	130		15.0	---	.42	.42	[b] 9.1×10^{-3}
	131		15.0	.25	.39	.36	14.4
	132		15.0	.28	.38	.36	13.2
	133		15.0	.20	.36	.32	12.7
Average[c]	---	----	----	0.28	0.40	0.39	12.8
2S[c] and symmetry[d]	---	----	----	.09 (3/2)	.08 (3/5)	.09 (3/5)	1.9 (2/4)

[a] f_1, 0 to 2 min; f_2, 10 to 15 min; f_A, 0 to 15 min.

[b] Deleted from average and statistics.

[c] Averages and S calculated from data at three significant figures.

[d] Number of specimens above average/number of specimens below average.

TABLE VIII. - COEFFICIENT OF SLIDING FRICTION FOR IRRADIATED SPECIMENS

Group	Specimen	Fast fluence ($E_n > 1.0$ MeV), neutrons/cm^2 (a)	Thermal fluence, neutrons/cm^2 (a)	Hours irradiated	Total f test run time, min	Coefficient of sliding friction[b]			Weight loss, kg
						f_1	f_2	f_A	
A	143	0.13×10^{20}	0.70×10^{20}	459	15.0	0.34	0.48	0.44	14.0×10^{-3}
	144	.12	.70	459	15.0	.32	.43	.40	14.0
B	101	1.1×10^{20}	5.8×10^{20}	910	18.3	----	0.42	0.42	[c]15.7
	103	1.0	5.7	910	16.1	0.29	.35	.33	[c]13.4
	105	1.2	5.7	910	15.0	.28	.37	.32	12.7
C	107	2.5×10^{20}	15×10^{20}	910	16.3	0.32	0.49	0.41	[c]11.7
	109	2.1	15	910	20.0	.31	.40	.38	[c]17.5
	111	3.6	14	910	20.0	.35	.42	.40	[c]15.9
D	102	2.8×10^{20}	15×10^{20}	2535	15.0	0.21	0.40	0.34	13.7
	104	2.8	15	2535	15.0	.23	.37	.34	12.0
	106	2.6	14	2535	15.0	.27	.42	.40	12.3
E	113	3.4×10^{20}	27×10^{20}	2535	15.0	0.19	0.30	0.38	14.4
	114	3.4	26	2535	15.0	.22	.35	.32	12.1
	115	3.5	26	2535	15.0	.30	.37	.35	14.7
F	108	9.1×10^{20}	64×10^{20}	4149	15.0	0.40	0.50	0.47	13.9
	110	10	63	4149	15.0	.40	.50	.48	12.3
	112	10	64	4149	15.0	.34	.40	.41	13.2
A to F average[d]	---	---------	-------	----	----	0.30	0.41	0.38	13.3
2S and symmetry[e]	---	---------	-------	----	----	.12 (8/7)	.10 (8/9)	.10 (9/7)	1.9 (6/6)
TC-1 and TC-2 average	---	---------	-------	----	----	.25	.39	.35	13.0
TC-1 and TC-2, 2S and symmetry	---	---------	-------	----	----	.09 (3/3)	.10 (2/4)	.10 (2/4)	1.7 (2/2)
AC-1 average	---	---------	-------	----	----	.28	.40	.39	12.8
AC-1 2S and symmetry	---	---------	-------	----	----	.09 (3/2)	.08 (3/5)	.09 (3/5)	1.9 (2/4)

[a]Dosimetry details and uncertainties are given in the appendix.

[b]f_1, 0 to 2 min; f_2, 10 to 15 min; f_A, 0 to 15 min.

[c]Deleted from averages and statistics.

[d]Averages and S calculated from data at three significant figures.

[e]Number of specimens above average/number of specimens below average.

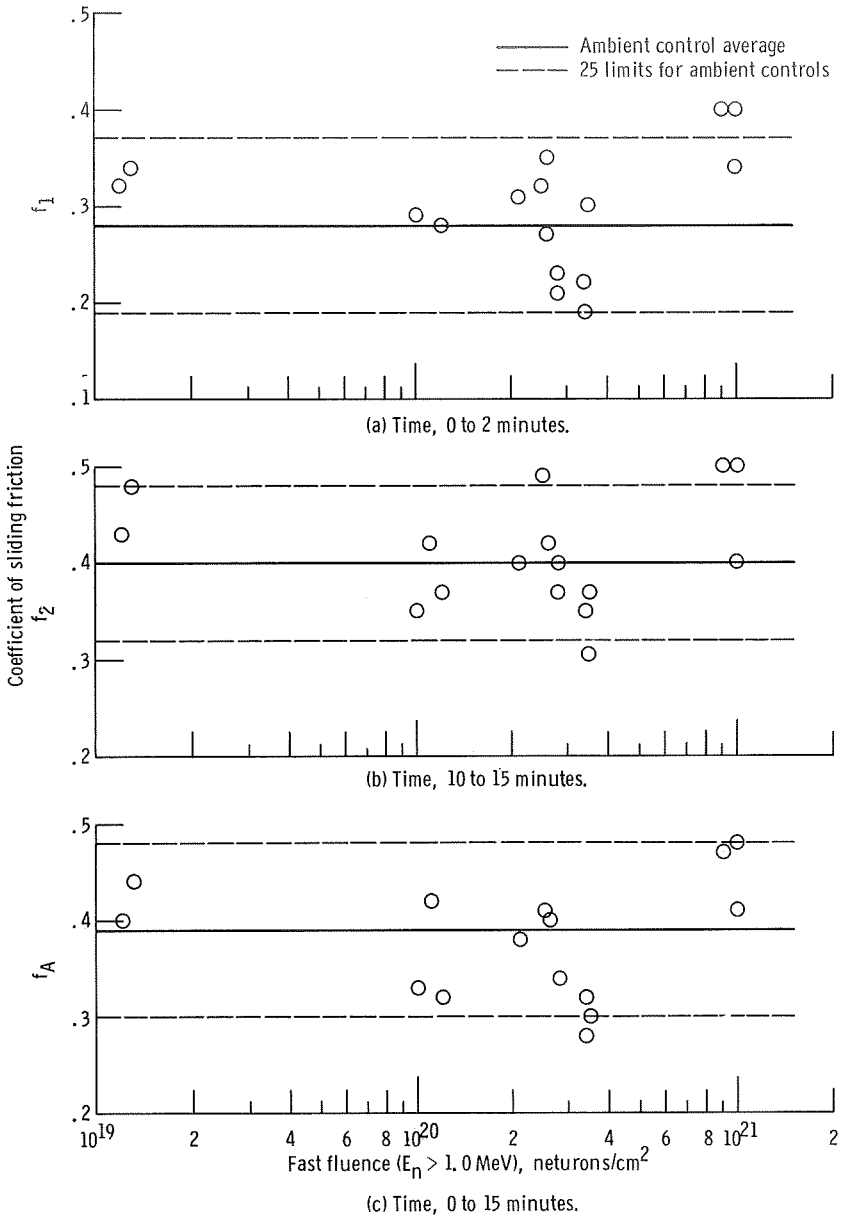

Figure 9. - Coefficient of sliding friction as function of fast neutron fluence.

group of F specimens may represent an increase in f at this fluence level or merely part of the statistical variation. Data beyond this fluence level or more data at this level would be required to reach a conclusion.

One can reach similar conclusions for f_2 based on arguments similar to those given for f_A. Four specimens fell outside the 2S uncertainty band for the ambient controls in this case.

The only differences noted in the behavior of f_1 as compared to f_2 and f_A was the degree of symmetry of the irradiated specimen values about the ambient control

average and the uncertainty in the irradiated specimen values. The distribution of the irradiated specimen values about the control average was biased on the high side (10/5). Also, the uncertainty in the average was slightly higher. Although the average for the irradiated specimens was slightly higher than for the controls, it was within the 1S uncertainty for the controls. The bias and larger uncertainty is most probably the result of the light, adherent deposit observed on some of the irradiated specimens. The dependence of f_1 on the initial surface condition of the specimens is certainly much greater than for f_2 or f_A.

The thermal controls showed slightly lower f's than the ambient controls. Again, the averages fell within the 1S uncertainty band for the ambient control average and cannot be considered significant. There is, however, a possible contributing factor, aside from a bona fide temperature effect. The temperature controls were exposed to 367 K water in a water bath. An analysis of this water at the termination of the thermal exposure showed a significant lead content. The heater guard was apparently made of a high lead alloy. A light deposit of lead on the specimen surface could certainly cause some reduction in f, especially f_1. It may be noted that f_1 showed the greatest decrease, which indicated that surface condition is probably the largest contributor to the lower f values.

Wear Rate

The total weight loss in a 15-minute period during the determination of f was used as the measure of wear rate. Therefore, those specimens run longer than 15 minutes were not included in this analysis.

A comparison of the wear data for the controls and irradiated specimens indicates that the irradiation had no effect on the wear rate (tables VII and VIII). This seems surprising at first since the Waukesha 88 was strengthened considerably during irradiation.

It is worth noting at this point that the Bi-Sn alloy, which acts as a lubricant, has a melting point of around 405 K. The nominal irradiation temperature was 355 K. This means that the irradiation temperature approximated 0.88 of the melting temperature. At this homologous temperature one would expect that radiation effects on the Bi-Sn alloy would anneal out as rapidly as they are formed. Thus the properties of the Bi-Sn alloy would remain essentially unchanged.

From this fact and the fact that no change in f was observed, one is led to the conclusion that it could basically be the properties of the Bi-Sn alloy that were measured during the f tests. Coupling this with the fact that no change was observed in the wear rate leads one to the further conclusion that the release of the Bi-Sn alloy is self-

regulating. The base alloy would wear at the rate required to maintain the optimum amount (giving minimum friction) of the lubricant at the sliding interface. It is necessary to assume, in this case, that the change in the properties of the base alloy does not affect the measured properties of the lubricant and its consumption rate at the interface.

There is one other mechanism that could explain the fact that there was no change in f or the wear rates. It was determined that the bulk temperature rise in the test specimens during testing was small. Although the exact temperatures were not measured, the control specimens were merely warm to the touch during testing. However, the temperatures of the asperities (high spots on the surface) can be quite high. And it is the properties of these asperities that primarily control the wear rate and f. If the temperatures of these asperities are sufficiently high, a nearly instantaneous local annealing of radiation damage might occur. The wear and friction properties would then be the same for irradiated material as for the controls. For complete annealing to occur, these temperatures must exceed 0.5 of the melting point of the alloy (1700 K), or approximately 850 K.

However, when the asperity temperatures reach 405 K, the Bi-Sn alloy will melt and moderate the asperity temperature. Also, the high asperity temperatures exist for very short periods of time ($\sim 10^{-4}$ sec). It is unlikely, then, that complete annealing would occur. There does remain the possibility, however, that the material properties at the asperity temperature might not be significantly different in the radiation damaged state from the unirradiated state.

Metallographic Examination

Figure 10 shows the microstructures of Waukesha 88 before and after irradiation. The specimens were etched with aqua regia. The globules of the Bi-Sn alloy are readily discernible in these photomicrographs. The unirradiated material did seem to be somewhat more sensitive to the etchant. No changes in microstructure are evident, and none would be expected at these fluences.

Autoradiography

Figure 11 shows the α and β-γ autoradiographs of the wear test disks for specimens 143 and 108, respectively. The α-graphs represent the distribution of the Bi-Sn alloy and the β-γ graphs show the distribution of the base metal.

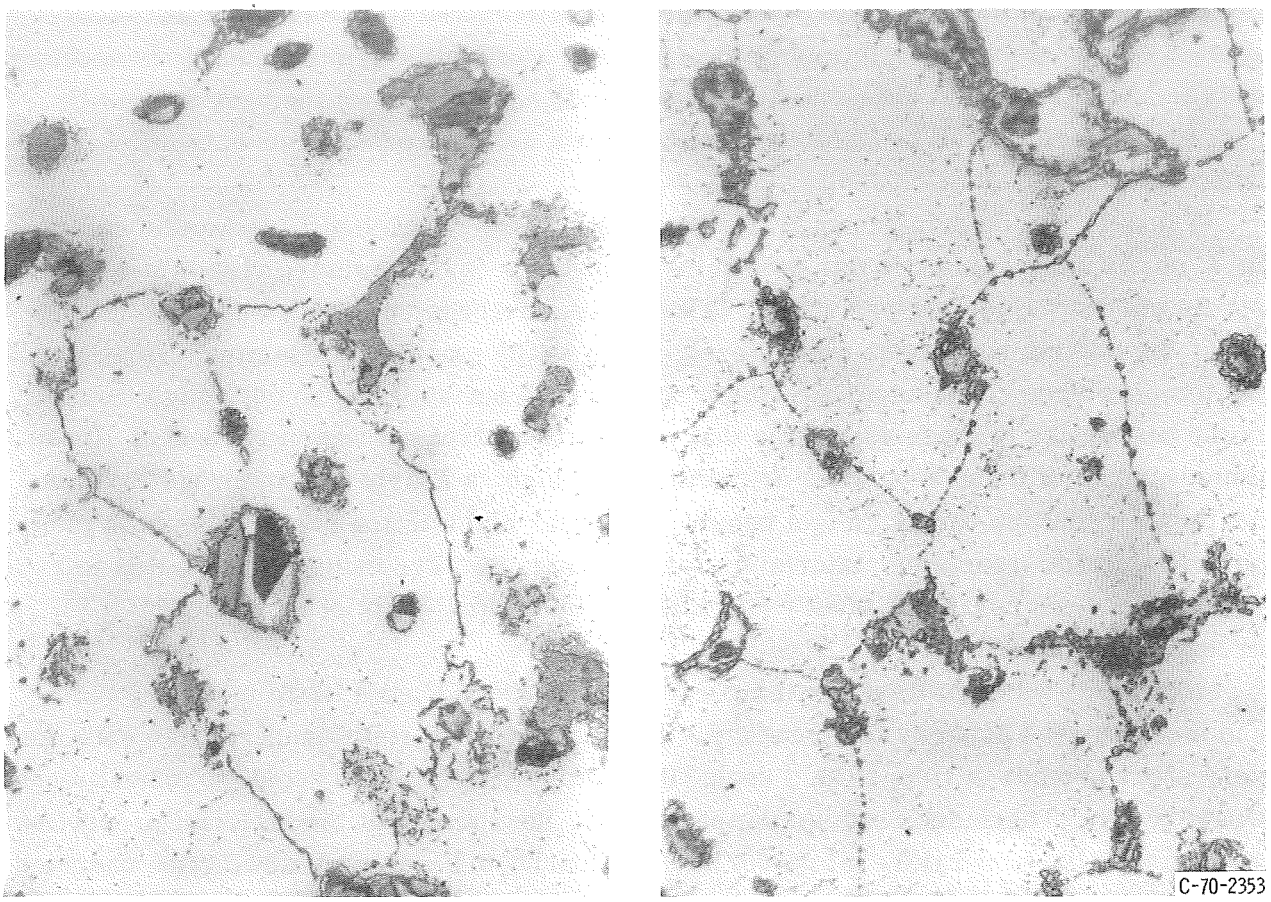

(a) Irradiated specimen 110.

(b) Thermal control specimen 122.

Figure 10. - Photomicrographs of Waukesha 88. Etched specimens. X500.

It is apparent that the lubricity or degree of smearing of the Bi-Sn alloy did not change with increasing fluence. This is not surprising since the irradiation temperature approximated 0. 88 of the melting temperature of the alloy. At this fraction of the melting point, irradiation effects would anneal out as rapidly as they were formed.

One might expect some differences in the appearance of the β-γ graphs with increasing fluence. The base metal undoubtedly had some ductility left at the lower fluence level. One might expect, therefore, to see a more streaked distribution on its wear disk than for the disk of the higher fluence specimen. However, no difference is apparent. From the granular appearance of these autoradiographs, it appears that the material release is of a more brittle than ductile nature in both cases.

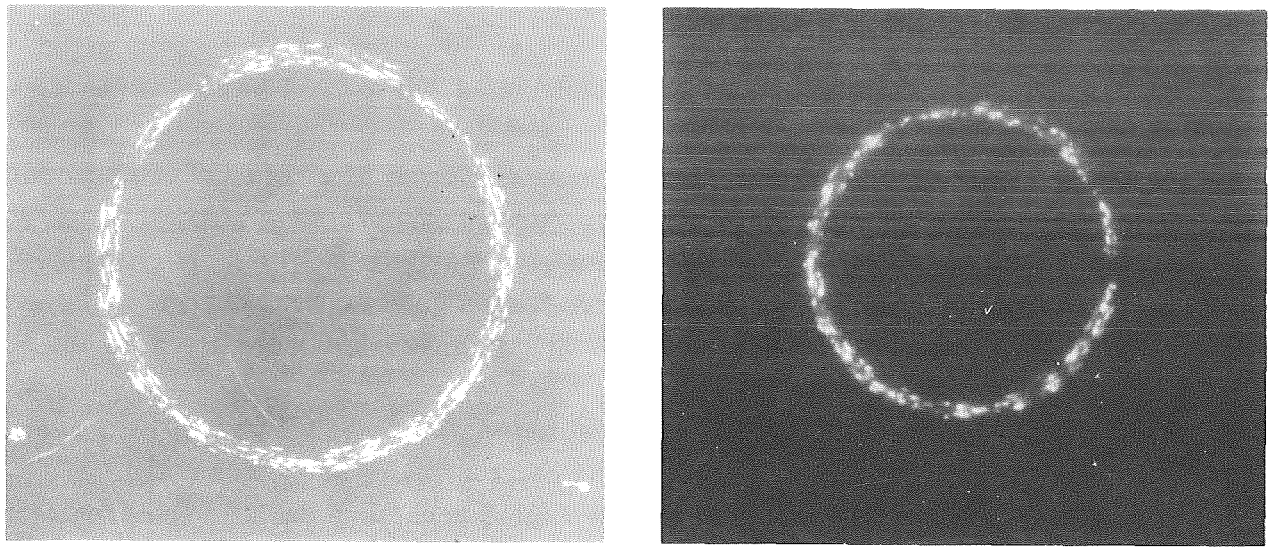

(a) Specimen 108.

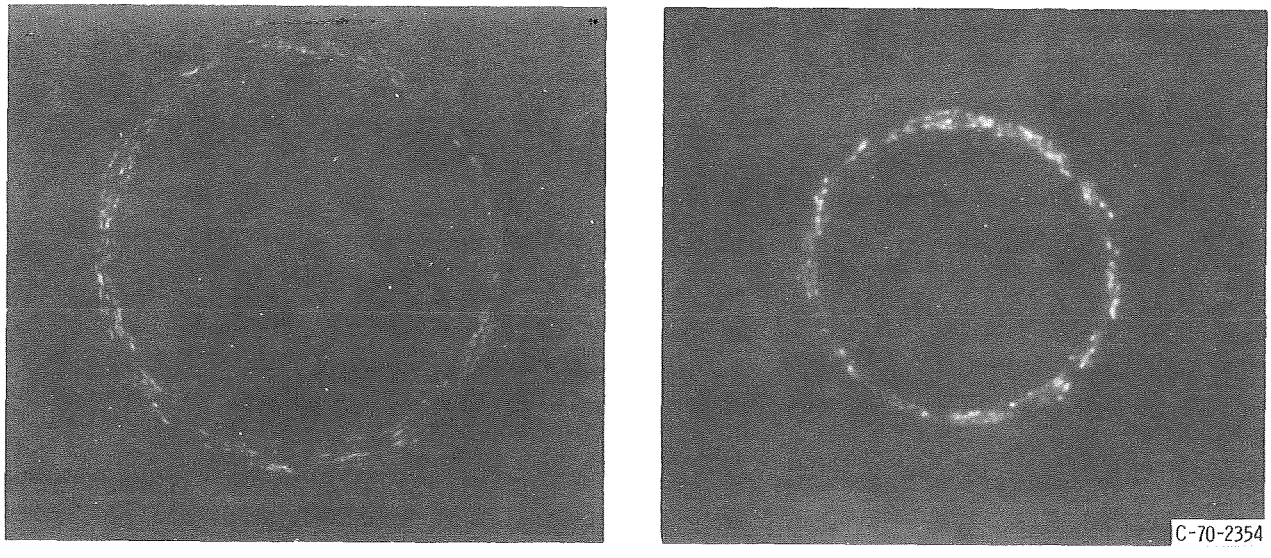

α graphs

β-γ graphs

(b) Specimen 143.

Figure 11. - α and β-γ radiographs of wear test disks.

CONCLUSIONS

The effects of radiation on the physical and mechanical properties of a nongalling alloy, Waukesha Metal 88, were determined up to a fast fluence of 1×10^{21} neutrons per square centimeter (neutron energy $E_n > 1.0$ MeV) at 355 K. The purpose of the evaluation was to determine the utility of this material in a radiation environment. The following observations were made:

1. The hardness increased from a Rockwell B of 80 to a Rockwell C of about 30.

2. The density decreased from 8.68×10^3 to 8.62×10^3 kilograms per cubic meter.

3. The ultimate tensile strength increased from 52 100 to 120 000 pounds per square inch (3.59×10^8 to 8.27×10^8 N/m^2).

4. The 0.2 percent offset yield strength increased from 37 100 to 120 000 pounds per square inch (2.56×10^8 to 8.27×10^8 N/m^2).

5. The coefficient of sliding friction against 304 stainless steel did not change.

6. The wear rate when sliding against 304 stainless steel did not change.

7. No galling tendencies when mated with 304 stainless steel were noted for the unirradiated or irradiated material.

8. The general corrosion resistance in deionized water was very good. However, some susceptibility to crevice corrosion in the reactor environment was noted.

It was concluded that the material is acceptable for use in a radiation environment up to 367 K and up to fast fluence of 1×10^{21} neutrons per square centimeter ($E_n > 1.0$ MeV). It was further concluded that its nongalling properties are not affected by a radiation environment at the fluences and temperatures mentioned.

Lewis Research Center,
National Aeronautics and Space Administration,
Cleveland, Ohio, July 7, 1970,
122-29.

APPENDIX - NEUTRON SPECTRA AND DOSIMETRY

Neutron Energy Spectra

The relative integral and differential neutron flux energy spectra are given in figures 12 and 13. These spectra were obtained by using one-dimensional 71 group diffusion calculations.

Dosimetry

The fast neutron fluence, ($E_n > 1.0$ MeV), was monitored by using nickel dosimeter wires. An effective cross section of 0.40 barn and a threshold of 2.9 MeV was used

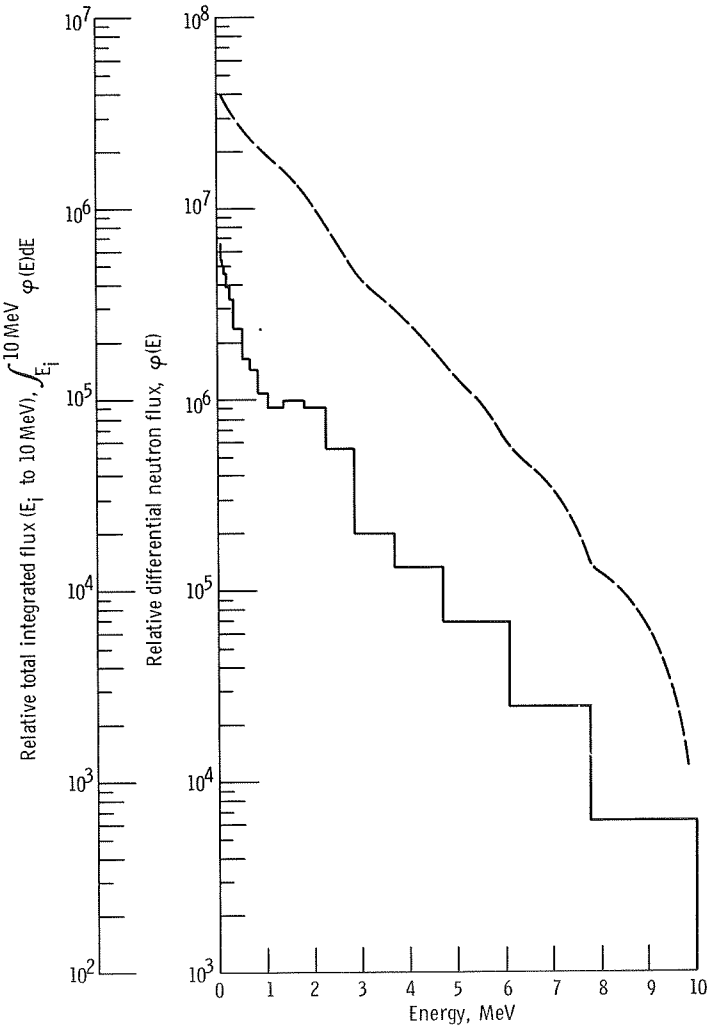

Figure 12. - Relative differential and integral flux values.

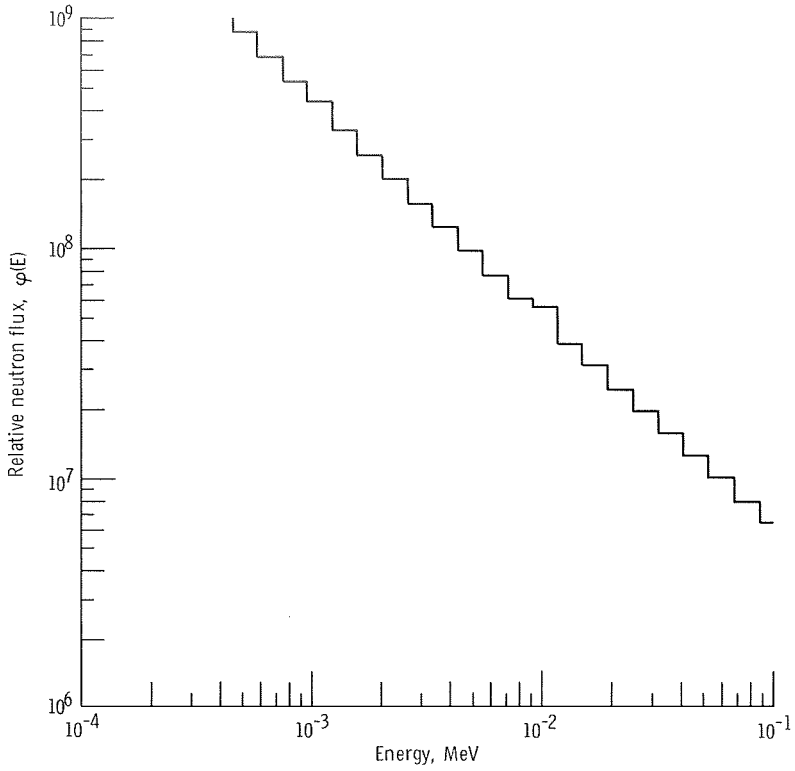

(a) Energy, 0.1 to 4.54×10^{-4} MeV.

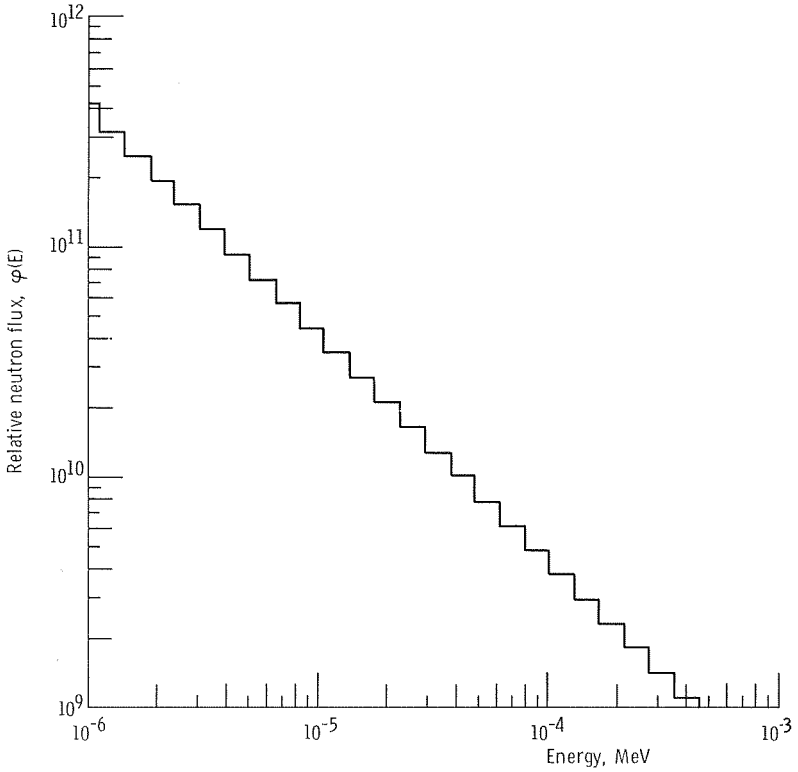

(b) Energy, 4.54×10^{-4} to 1×10^{-6} MeV.

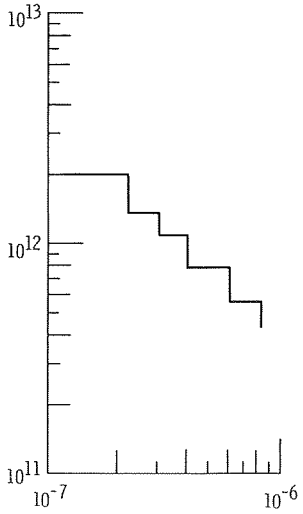

(c) Energy, 1×10^{-6} to 1.19×10^{-7}

Figure 13. - Relative differential neutron flux values.

for the $Ni^{58}(n, P)Co^{58}$ reaction. The thermal neutron fluence was monitored with cobalt wires using a cross section of 37.2 barns for the $Co^{59}(n, \gamma)Co^{60}$ reaction. The neutron flux, energy > X, may be determined by using the reported values for $\varphi f(E_n > 1.0$ MeV) and the relative integral flux values from figure 12. Thus,

$$\varphi(E > X) = \frac{\text{Relative } \varphi(E > X) \times \varphi f(E > 1.0)}{\text{Relative } \varphi(E > 1.0)}$$

The positions of the dosimeter wires and specimens in a typical capsule segment are shown in figure 14. One cobalt and one nickel wire were at each dosimeter position. The neutron fluence at the specimen midpoint for a typical specimen in position 6A was calculated using the dosimeters from positions 6a, 6c, 5a, and 5c and assuming all gradients were linear. The uncertainty introduced by this method is ±10 percent. The uncertainty was determined from data collected in the Plum Brook Mockup Reactor, in which dosimeter wires were also placed at the specimen midpoints.

The uncertainties in the fluence values are given in table IX.

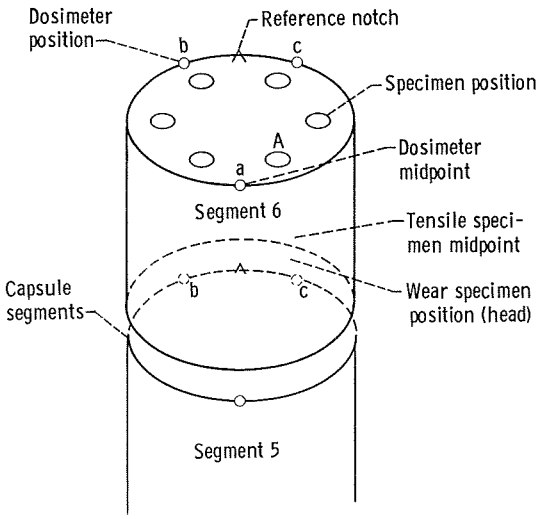

Figure 14. - Relative positions of dosimeter wires and specimens in capsule.

TABLE IX. - UNCERTAINTIES IN NEUTRON FLUENCES

Neutron energy, E_n, MeV	Uncertainty (95 percent confidence), percent	
	At dosimeter position	At specimen midpoint
>1.0	±22	±24
>.1	±41	±42
Thermal	±10	±14

REFERENCES

1. Fecych, William: Experiences with Beryllium Swelling and Replacement in the Plum Brook Reactor. Presented at the American Nuclear Society Winter Meeting, Washington, D. C., Nov. 11-16, 1968.
2. Paine, S. H.; Murphy, W. F.; and Hackett, D. W.: A Study of Irradiation Effects in Type "A" Nickel and Type 347 Stainless Steel Tensile Specimens. Rep. ANL-6102, Argonne National Lab., July 1960.
3. Smith, Karl F.: Stainless Steels. Materials. Vol. 1 of Reactor Handbook. C. R. Tipton, Jr., ed., Interscience Publ., Inc., 1960, p. 563.
4. Bush, Spencer H.: Irradiation Effects in Cladding and Structural Materials. Rowman and Littlefield, Inc., 1965.
5. Cummings, W. V.: X-ray Diffraction Studies of Defect Structures in Irradiated Metals. J. Phys. Soc., Japan, vol. 18, Suppl. III, 1963, pp. 189-194.
6. Tucker, W. C., Jr.; and Sampson, J. B.: Interstitial Content of Radiation Damaged Metals from Precision X-ray Lattice Parameter Measurements. I. Principles of the Measurements. Rep. KAPL-1037, Knolls Atomic Power Lab., Jan. 26, 1954.

NASA-Langley, 1970 —— 17 E-5704

NATIONAL AERONAUTICS AND SPACE ADMINISTRATION
WASHINGTON, D.C. 20546

OFFICIAL BUSINESS

FIRST CLASS MAIL

POSTAGE AND FEES PAID
NATIONAL AERONAUTICS AND
SPACE ADMINISTRATION

POSTMASTER: If Undeliverable (Section 158 Postal Manual) Do Not Return

"The aeronautical and space activities of the United States shall be conducted so as to contribute . . . to the expansion of human knowledge of phenomena in the atmosphere and space. The Administration shall provide for the widest practicable and appropriate dissemination of information concerning its activities and the results thereof."

—NATIONAL AERONAUTICS AND SPACE ACT OF 1958

NASA SCIENTIFIC AND TECHNICAL PUBLICATIONS

TECHNICAL REPORTS: Scientific and technical information considered important, complete, and a lasting contribution to existing knowledge.

TECHNICAL NOTES: Information less broad in scope but nevertheless of importance as a contribution to existing knowledge.

TECHNICAL MEMORANDUMS: Information receiving limited distribution because of preliminary data, security classification, or other reasons.

CONTRACTOR REPORTS: Scientific and technical information generated under a NASA contract or grant and considered an important contribution to existing knowledge.

TECHNICAL TRANSLATIONS: Information published in a foreign language considered to merit NASA distribution in English.

SPECIAL PUBLICATIONS: Information derived from or of value to NASA activities. Publications include conference proceedings, monographs, data compilations, handbooks, sourcebooks, and special bibliographies.

TECHNOLOGY UTILIZATION PUBLICATIONS: Information on technology used by NASA that may be of particular interest in commercial and other non-aerospace applications. Publications include Tech Briefs, Technology Utilization Reports and Notes, and Technology Surveys.

Details on the availability of these publications may be obtained from:

SCIENTIFIC AND TECHNICAL INFORMATION DIVISION

NATIONAL AERONAUTICS AND SPACE ADMINISTRATION

Washington, D.C. 20546